An Extended Two-Point Dixon Algorithm for Calculating Separate Water, Fat, and B_0 Images

Thomas E. Skinner, Gary H. Glover

A new algorithm is presented that provides separate water, fat, and B_0 images utilizing the in-phase and opposed-phase acquisitions of the two-point Dixon (2PD) method. The accuracy of the extended method (E2PD) compares favorably with the three-point Dixon (3PD) method, and the acquisition requires 2/3 the 3PD scan time. Slightly increased mismapping may occur in pixels containing an admixture of water and fat due to reduced SNR in the B_0 field map compared with the 3PD method.

Key words: Dixon methods; water-fat imaging.

INTRODUCTION

Chemical shift resolution in MRI entails the capability of differentiating between water and fat, which dominate the *in vivo* human proton spectrum. Methods that suppress either the water (1) or fat (2–4) signal before acquisition represent one possible strategy for achieving this end. However, the accuracy of these methods depends sensitively on the homogeneity of the polarizing field B_0. Moreover, the effect of B_0 inhomogeneity on the performance of these techniques is not readily corrected during acquisition. An alternative method, originally developed by Dixon (5), is based on the strategy of achieving the water/fat separation after signal acquisition. This technique acquires two separate images with the water and fat magnetizations in-phase and opposed. If the B_0 field is uniform, these two components can be unraveled by adding and subtracting the resulting images. However, the orientation of the net water/fat magnetization vector in each pixel of the opposed-phase image depends on B_0, so the simple Dixon method is also sensitive to B_0 homogeneity.

To address this limitation of the two-point Dixon (2PD) method, the three-point Dixon (3PD) method was developed (6) and subsequently generalized (7) to allow determination of the B_0 map as well as a measurement of intravoxel susceptibility dephasing in each pixel using the extra measurement points. With the field known at each pixel, an ideal decomposition can be achieved to provide separate water and fat images. Unfortunately, these N-point Dixon methods require a concomittantly longer acqusition time than an unresolved image, which often limits their application in many practical situations.

In this Note, we observe that under certain conditions, an accurate field map can be obtained without the third acquisition, thereby providing separate water, fat, and B_0 images with 2/3 the scan time of the 3PD method. Only the in-phase and opposed-phase images are acquired as in the simple 2PD method, but a new postprocessing step is utilized to effect the decomposition. The new technique is called an extended two-point Dixon method (E2PD). It is compared with current 3PD methods and is shown to provide a viable alternative in cases where reduction of the total imaging time is a higher priority than optimal accuracy of the decomposition. An example where the two methods produce indistinguishable results is also provided.

METHODS

The description of the extended two-point method closely follows the treatment given in ref. 6. Examples of both spin echo and gradient recalled echo versions of the

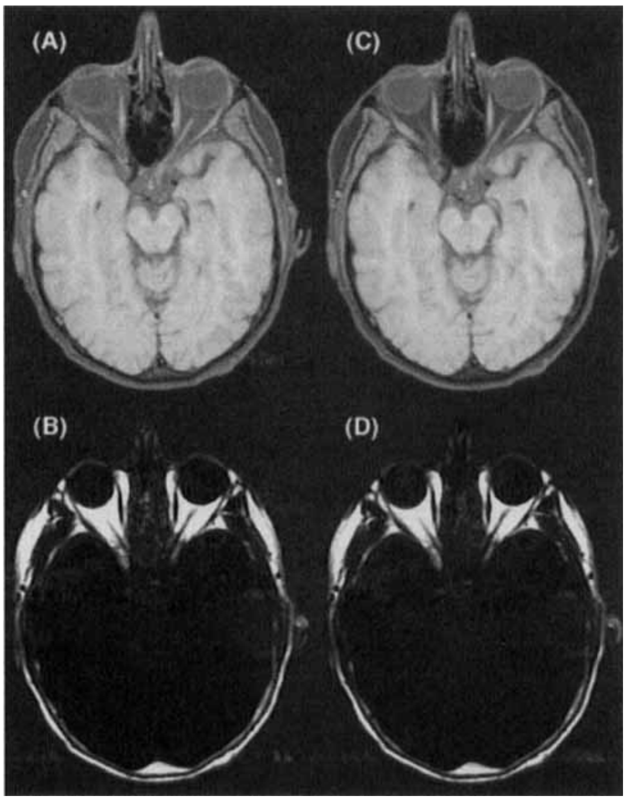

FIG. 1. Extended two-point Dixon (E2PD) method ((A) water, (B) fat) and corresponding images for the three-point Dixon method (C, D). Few differences are apparent, with an exception noted in the left ear, where phase unwrap failures cause transposition of the fat and water.

MRM 37:628–630 (1997)

From the Physics Department, Wright State University, Dayton, Ohio (T.E.S.) and Department of Radiology, Stanford University, Stanford, California (G.H.G.).

Address correspondence to: Thomas E. Skinner, Ph.D., Physics Department, Wright State University, Dayton, OH 45435.

Received June 17, 1996; revised September 13, 1996; accepted September 16, 1996.

0740-3194/97 $3.00

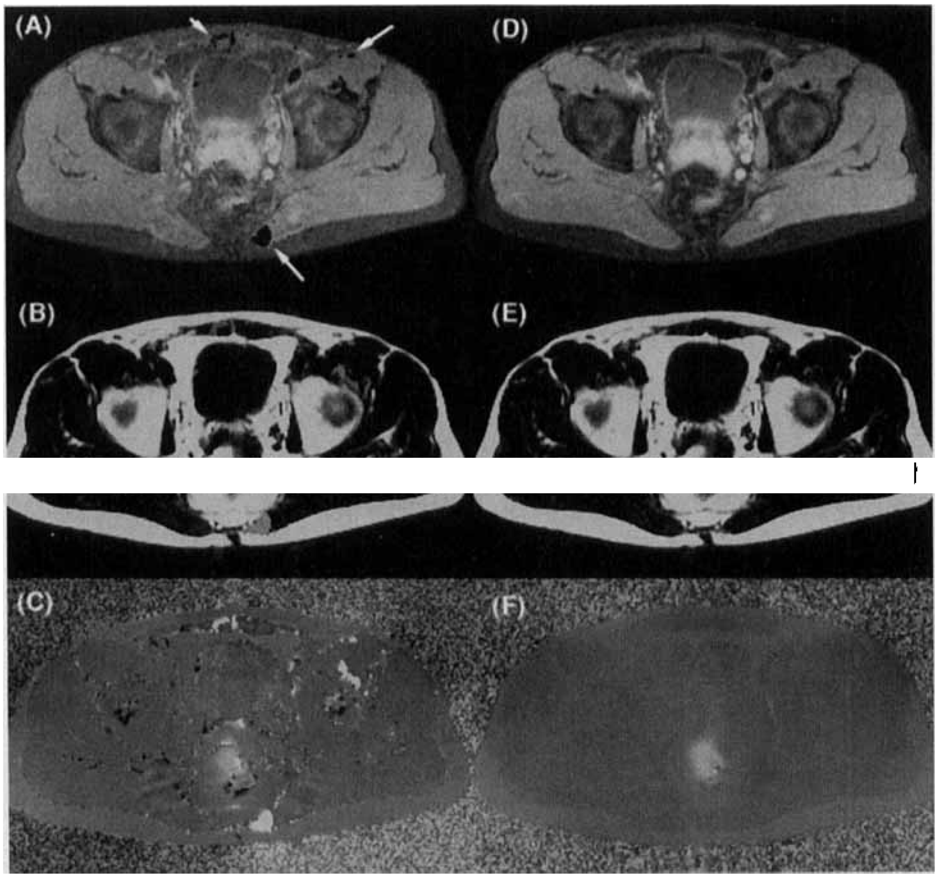

FIG. 2. (A-C) Extended two-point Dixon (E2PD) method, showing water, fat and B_0 maps, respectively. (D-F) Corresponding images for the three-point Dixon method. Arrows show regions where the E2PD decomposition fails due to an improper B_0 map (compare (C) and (F)) for voxels containing nearly equal amounts of water and fat, as described in the text.

basic pulse sequence required for Dixon acquisitions can be found in Fig. 3 of ref. 7. Two images are acquired with respective phase shifts of 0 and π between the water and fat components. The first image, denoted S_0, is obtained conventionally, while the second image (S_1) is acquired by shifting either the 180° pulse or refocusing gradient by a time $\tau/2$ or τ, respectively, where $\tau = \pi/\omega_c$, with ω_c the fat/water chemical shift. The amplitudes of the water and fat components that are to be determined are written as ρ_1 and ρ_2, respectively. The systematic phase offset that is produced in each voxel as a result of RF penetration effects and other phase accumulations that are independent of chemical shift is denoted by ϕ_0. This is the only phase component in S_0, since chemical shift evolution and magnetic field inhomogeneity are refocused in this acquisition. B_0 field variation produces an additional phase ϕ in each component of S_1 given by

$$\phi = \omega_0 \tau = \pi \omega_0 / \omega_c \quad [1]$$

where ω_0 is the offset frequency. Voxel intensities in the two complex images can therefore be written as

$$S_0 = (\rho_1 + \rho_2) e^{i\phi_0} \quad [2]$$

$$S_1 = |\rho_1 - \rho_2| e^{i(\phi + \phi_0)} \quad [3]$$

The original Dixon method implicitly assumes $\phi = 0$ to consider a solution $\rho_{1,2}\, e^{i\phi_0} = (S_0 \pm S_1)/2$. In pixels where $\phi \neq 0$, the final decomposition is an admixture of fat and water, depending on the value of ϕ. Severe phase artifacts are produced in the final image as a result of ϕ_0 variation throughout the image and the false assumption of uniform B_0 field. Therefore, as noted previously (6), magnitude images were used in the original 2PD decomposition to obtain $\rho_{1,2} = (\,|S_0| \pm |S_1|\,)/2$. In addition to the loss of SNR inherent in this procedure, an accurate water/fat separation is obtained with this method only if $\rho_1 > \rho_2$ throughout the image. Yet, there is sufficient information in the two acquired images to provide a more satisfactory solution.

Since ϕ_0 is available immediately as the argument of S_0, Eqs. [2]–[3] are conveniently rewritten as (6)

$$S_0' = \rho_1 + \rho_2 \quad [4]$$

$$S_1' = |\rho_1 - \rho_2| e^{i\phi} \quad [5]$$

with

$$S_n' = S_n e^{-i\phi_0}$$

The argument of S_1' in Eq. [5] can be found only to within π since the sign of $\rho_1 - \rho_2$ is not known, but 2ϕ

can be found unambiguously as the argument of $(S_1')^2$. The algorithm for determining the absolute phase ϕ' corresponding to the principal value of 2ϕ was developed in ref. 8. The absolute phase for ϕ is then determined as $\phi'/2$. The sign of $\rho_1 - \rho_2$ can then be determined from the sign p of $S_1'e^{-i\phi}$. In fact, the argument of $S_1'e^{-i\phi}$, which should be either 0 or π, measures the accuracy of ϕ determined in the previous step and can be used to adjust this parameter. Finally, the water and fat components are obtained as

$$\rho_{1,2} = (S_0' \pm pS_1'e^{-i\phi})/2 \quad [6]$$

RESULTS AND DISCUSSION

A comparison of the E2PD and 3PD methods is shown in Fig. 1 for a brain slice. Three-point Dixon T_1-weighted spin echo images were obtained with 0, π, and 2π fat-water phase shifts (*TR/TE* 500/11 ms, 192 × 256 matrix, 5 mm slice). Figures 1A and 1B were reconstructed with the E2PD method by using only the 0 and π images while Figs. 1C and 1D used the conventional 3PD method. The decompositions for both methods are nearly identical.

Figure 2 shows a similar comparison for a pelvic slice. Figures 2A–2C were reconstructed with the E2PD method by using only the 0 and π images; Figs. 2D–2F used the conventional 3PD method. In this case, the E2PD decomposition has regions in which water and fat are interchanged (arrows, and compare Figs.2A and 2D). The errors tend to occur in regions bordering fat-water boundaries, and derive from an improper B_0 map, as is evident in Fig. 2C compared with Fig. 2F. The SNR in the E2PD B_0 map is low in the fat/water boundary regions because the signal in the opposed phase map tends toward zero, and because the phase difference is half that of the 3PD method. The 3PD method uses two in-phase images to calculate the B_0 map, and therefore does not have signal dropout in pixels with an admixture of water and fat.

In addition to the greater potential for errors from field mismapping, a second difference between the E2PD and 3PD methods is that the lipid signal is less well suppressed in the two-point method, as may be seen by comparing the subcutaneous fat in Figs. 2A and 2D. This results from the fact that the fat "line" is broadened from the inequivalent fatty acid constituents, which in turn causes a T_2* decay in the shifted-echo acquisitions (7). The lipid signal loss for a 2π acquisition is approximately twice that for a π acquisition. With the three-point method, the 0 and 2π signals are averaged together, and thus the combined lipid intensity loss nearly balances that for the π acquisition. With E2PD, however, there is an unbalanced lipid signal loss in the π acquisition relative to the 0 acquisition, and thus the decomposition does not suppress the fat signal as completely.

CONCLUSIONS

In summary, the E2PD method functions nearly as well as the 3PD method in cases where the SNR is high enough to preclude phase unwrap errors in the intrinsically lower quality E2PD field map and where the slight loss of fat suppression is not troublesome. The E2PD method should find use in a variety of applications for which the longer 3PD method is precluded. The algorithm has been found to work well with gradient echoes or spin echoes, and can be readily implemented in a RARE (9) sequence, as demonstrated previously (10) using 3PD.

REFERENCES

1. A. Haase, J. Frahm, Multiple chemical-shift-selective NMR imaging using stimulated echoes. *J. Magn. Reson.* **64,** 94–102 (1984).
2. P. J. Heller, W. W. Hunter, P. Schmalbrock, Multisection fat-water imaging with chemical shift selective presaturation. *Radiology* **164,** 539–541 (1987).
3. J. Szumowski, D. B. Plewes, Fat suppression in the time domain in fast MR imaging. *Magn. Reson. Med.* **8,** 345–354 (1988).
4. J. Mao, H. Yan, W. D. Bidgood, Fat suppression with an improved selective presaturation pulse. *Magn. Reson. Imaging* **10,** 49–53 (1992).
5. W. T. Dixon, Simple proton spectroscopic imaging. *Radiology* **153,** 189–194 (1984).
6. G. H. Glover, E. Schneider, Three-point Dixon technique for true water/fat decomposition with B_0 inhomogeneity correction. *Magn. Reson. Med.* **18,** 371–383 (1991).
7. G. H. Glover, Multipoint Dixon technique for water and fat proton and susceptibility imaging. *J. Magn. Reson. Imaging* **1,** 521–530 (1991).
8. S. Moon-Ho, S. Napel, N. J. Pelc, G. H. Glover, Phase unwrapping of MR phase images using Poisson equation. *IEEE Trans. Image Proc.* **4,** 667–676 (1995).
9. J. Hennig, A. Naureth, H. Friedburg, RARE imaging: A fast imaging method for clinical MR. *Magn. Reson. Med.* **3,** 823–833 (1988).
10. P. A. Hardy, R. S. Hinks, J. A. Tkach, Separation of fat and water in fast spin-echo MR imaging with the three-point Dixon technique. *J. Magn. Reson. Imaging* **5,** 181–185 (1995).